and 68 amu. The intensity ratios of the two product ions are different between TMAO and d_9-TMAO due to the difference in bond energy among C and H and C and D (deuterium). We therefore quantified TMAO and d_9-TMAO in the MRM mode using the precursor to product transitions 76 → 58 and 85 → 66 amu, respectively. Among all the instrument parameters, collision energy (CE) was the most critical one.

Validation of the LC/MS/MS assay for TMAO in human plasma

Fig. 2A and B shows the selected ion extraction LC chromatograms of TMAO and d_9-TMAO standards (in buffer) in positive MRM mode. Fig. 2C and D shows the LC chromatograms extracted in plasma after spiking with d_9-TMAO internal standard in methanol followed by precipitation to remove protein. TMAO and d_9-TMAO have nearly the same retention times in the LC chromatograms. The data acquisition window is 6 min, and began after an initial 4.5 min of column eluent diversion to waste. To increase sample throughput, we routinely use 2 multiplexed binary pump HPLC system equipped with separate columns and automated column valve system [10], allowing for data acquisition only during a narrower time window from each column (Fig. 3). The current column and gradient presented are what we typically use, and allows for an ~11 min per sample run time, while also allowing multiple additional biogenic amines and amino acids to simultaneously be quantified in multiple reaction monitoring mode [11]. If only quantifying TMAO, we increase throughput per sample to ~5 min by using a shorter column and gradient (not shown). Following data acquisition, peak areas of TMAO and d_9-TMAO were determined using Analyst 1.4.1 software and the peak area ratio is used to quantify TMAO. Using a series of concentrations of TMAO standard mixed with a fixed amount of d_9-TMAO internal standard spiked or nonspiked into plasma, we prepared calibration curves, which are shown in Fig. 4A and B. The *Y* axis intercept in Fig. 4B (nondialyzed plasma) corresponds to the endogenous TMAO concentration, which can be calculated as intercept/slope. The slopes of the two standard curves showed a difference of ⩽3.2%. By spiking a series of concentrations of TMAO standards into 8 different plasma samples to prepare the standard curves, we got a slope (mean ± SD) of 0.0156 ± 0.0003, suggesting that using different spiked plasmas to generate the calibration curves for TMAO gives an error of ⩽2.0%. These data also indicate that in either EDTA plasma (shown) or serum (not shown) the matrix effect for quantifying TMAO by the method described is negligible.

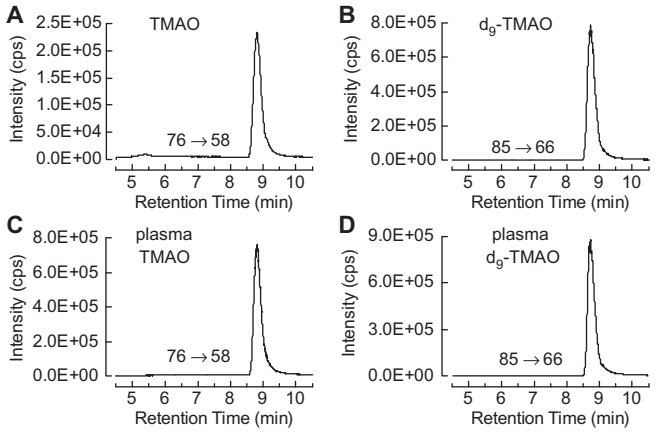

Fig.2. Detection of TMAO in biological matrices. Extracted-ion LC chromatograms from multiple reaction monitoring in positive-ion mode of TMAO (A), d_9-TMAO (B), standards and plasma (C and D), spiked with 4 vol of internal standard, d_9-TMAO, at a concentration of 10 μM in methanol. The precursor-to-product transitions were 76 → 58 and 85 → 66 amu, respectively. Note, prior to data collection, the eluent was diverted to waste for the initial 4.5 min of the gradient. The concentrations of TMAO in standard (A) and plasma (C) were 20.0 and 56.9 μM, respectively.

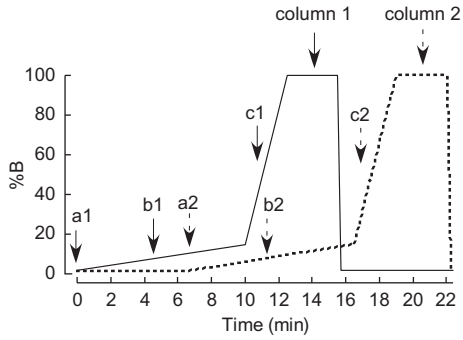

Fig.3. Multiplex binary gradient elution profile for quantitation of trimethylamine-*N*-oxide (TMAO) by LC/MS/MS. Two different solvents, A, 0.1% propanoic acid in water, B, 0.1% acetic acid in methanol, were used to generate the gradient. a1 and a2, time point for sample injection on columns 1 and 2, respectively; b1 and b2, time point for start of data collection on columns 1 and 2, respectively; c1, c2, time point for data collection to end and column 1 and 2 to be switched to waste, respectively.

Assay performance metrics

To examine assay precision, TMAO concentration was measured in 6 different pooled plasma samples with different TMAO levels, on multiple different days. Table 1 shows the intraday and interday CV%s for TMAO observed, all of which were less than 6.4 and 9.9, respectively, regardless of the TMAO level. The pooled plasma TMAO concentrations used were as low as 0.82 μM and as high as 102.4 μM, whose range embraces 99% subjects (see below). Additional assay performance metrics including accuracy across a span of different concentrations of TMAO (all ⩾95%), LLOD, LLOQ, and ULOQ are given in Table 2. The LC chromatogram of the TMAO standard spiked into the dialyzed plasma with a concentration at LLOQ is shown in Fig. 5A. Fig. 5B shows the LC chromatogram of TMAO in human plasma with the lowest concentration (0.06 μM) we have ever measured among more than 4000 subjects. The assay was found to be linear across the range examined (0.1–200 μM). Dilution of plasma samples containing higher TMAO levels (the highest endogenous level yet observed is 4.8 mM) with water gave an accuracy of greater than 98%.

Normal range of fasting plasma TMAO in healthy subjects

To assess the normal range of fasting (⩾12 h) TMAO levels, apparently healthy subjects (n = 349) undergoing routine health screens in the community were examined. Fig. 6A shows the plasma TMAO concentration distribution, and Table 3 describes the clinical and laboratory characteristics observed. Within the healthy cohort, 5% demonstrated mild hypertension and 5% of them were current smokers. The median (interquartile range) levels of TMAO noted was 3.45 (2.25–5.79) μM. Male and female TMAO levels showed no significant differences, though TMAO levels did show increases with age (Fig. 6B).

Stability studies

In order to investigate the stability of TMAO in plasma during storage, we measured TMAO concentrations in a collection of samples in which initial levels were determined using stable isotope dilution LC/MS/MS analyses over 5 years ago, and for which samples had been maintained at −80 °C. Fig. 7 shows results of the comparison in TMAO levels between the two time points, and

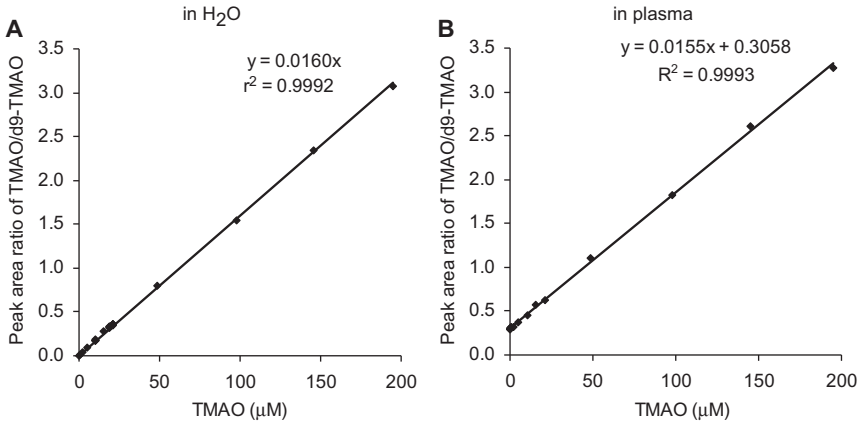

Fig.4. Standard curves for LC/ESI/MS/MS analysis of TMAO. 80 μl 10 μM d_9-TMAO internal standard in methanol was added to 20 μl different concentrations of TMAO standard (A) or 20 μl control plasma (B) spiked with different concentrations of TMAO standard followed by spin-down to remove precipitated protein. Analyses were performed using electrospray ionization in positive-ion mode with multiple reaction monitoring of precursor and characteristic product ions. The transitions monitored were mass-to-charge ratio (*m/z*): *m/z* 76 → 58 amu for TMAO; and *m/z* 85 → 66 amu for d_9-TMAO. Standard curves of TMAO were generated by plotting peak area ratio versus the concentration in water or spiked into plasma.

Table 1
Precision of TMAO concentrations measured in 6 pooled plasma samples with different levels over a span of more than 20 days.

Pooled plasma	Mean ± SD	Intraday CV%	Interday CV%
1	0.82 ± 0.05	6.4	5.8
2	1.68 ± 0.10	4.1	9.9
3	2.95 ± 0.11	3.1	5.8
4	2.44 ± 0.09	2.7	6.1
5	66.8 ± 2.1	2.1	5.2
6	102.4 ± 3.3	1.3	6.2

The calculated mean, SD, intraday CV% and interday CV% are given. For each of the 6 different plasma samples, a cluster of 4 determinations is presented as they were run on eight separate days (32 determinations total for each pooled plasma sample).

Table 2
Characteristics of the method for TMAO determination by LC/MS/MS.

Characteristic		Value
LLOD		0.02 μM
LLOQ		0.05 μM
ULOQ		>200 μM
Accuracy (%)	0.5 μM	98.2
	2 μM	97.1
	5 μM	97.3
	100 μM	101.6
	200 μM	97.4

Lower limit of detection (LLOD) = 3:1 signal to noise, Lower limit of quantitation (LLOQ) = 10:1 signal to noise, Upper limit of quantitation (ULOQ) = greater than highest standard investigated, Accuracy = ratio of the TMAO concentration measured to the TMAO concentration added to a dialyzed plasma sample.

reveals a high correlation (r^2 = 0.98) with slope and *Y* intercept very close to 1 and 0, respectively, indicating that TMAO is stable during storage at −80 °C. Separate studies examining the stability of TMAO through multiple freeze thaw cycles showed that TMAO levels do not significantly change, with intercycle CV% less than 10 (Table 4).

Discussion

Herein we present an LC/MS/MS method for the measurement of TMAO levels in biological matrices with high accuracy, precision, and throughput that is amenable to the demands of clinical

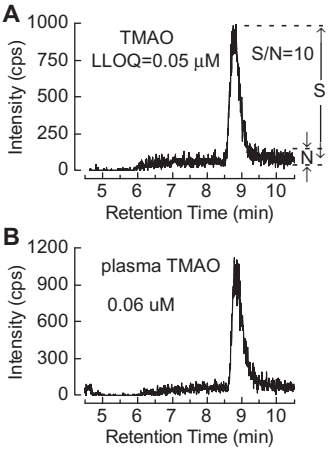

Fig.5. (A) Extracted-ion LC chromatogram at the LLOQ from multiple reaction monitoring in the positive mode of the 76 to 58 amu precursor to product ions from 0.05 μM TMAO standard spiked to dialyzed plasma; note this gives a signal-to-noise ratio (S/N) of 10: 1. (B) Extracted-ion LC chromatogram recorded as above of the plasma TMAO level at the lowest concentration (0.06 μM) among the more than 4000 human samples analyzed.

diagnostic practice. Using multiplexed HPLC with column switching, shorter column, and further optimization of the column gradients, we have adapted the stable isotope dilution LC/MS/MS assay described to permit a between sample acquisition time of 5 min (averaged) without affecting assay results or the column longevity. With a LLOQ of 0.05 μM, which is well below the lowest TMAO level observed among the >300 healthy volunteers examined, a highly accurate TMAO level was able to be determined in every subject examined. The linear relationship observed across the large dynamic range explored in the standard curve (up to 200 μM) is suitable for the majority of samples in human population studies. In our experience, which cumulatively includes analyses of over 4000 individuals (both healthy subjects and cardiovascular disease patients), the lowest plasma TMAO level observed thus far has been 0.06 μM (Fig. 5B), which is higher than the LLOQ, and the maximum level observed has been 4.8 mM. In the present studies, which report for the first time the normal range of fasting plasma TMAO levels among apparently healthy adult subjects, plasma TMAO levels at the 0.5 percentile level cutoff were 0.78 μM and at the 99.5 percentile cutoff were 46.0 μM. Previously, we mea-

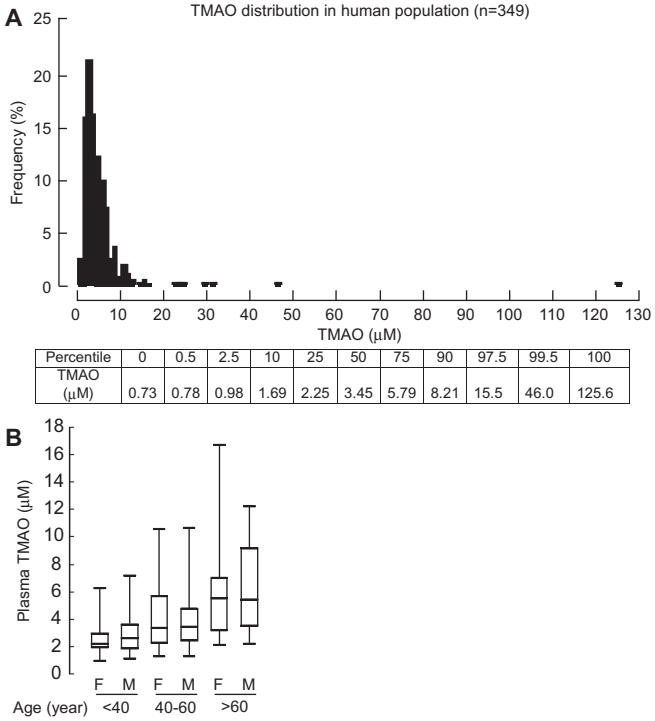

Percentile	0	0.5	2.5	10	25	50	75	90	97.5	99.5	100
TMAO (μM)	0.73	0.78	0.98	1.69	2.25	3.45	5.79	8.21	15.5	46.0	125.6

Fig.6. (A) Distribution of TMAO concentrations in healthy volunteers ($n = 349$). Lower bar gives the concentrations of TMAO at each percentile. (B) Box whisker plot showing distribution of the TMAO concentration with respect to age and gender in the above population ($n = 349$). The population was segregated by age and gender as shown on the lower axis. Horizontal in middle of box = TMAO concentration at median value, top of box at 75th percentile, bottom of box at 25th percentile, top of whisker at 97.5 percentile, and bottom of whisker at 2.5 percentile in the specified population.

Table 3
Clinical and laboratory characteristics of healthy controls.

Characteristic	All participants ($n = 349$)
Age–years	54 ± 16
Male sex–%	33
Median body-mass index (interquartile range)	25 (23–29)
Hypertension–%	5
Current or former smoker–%	5
Median cholesterol (interquartile range)–mg/dl	
Low-density lipoprotein	117 (95–142)
High-density lipoprotein	53 (45–64)
Median triglycerides (interquartile range)–mg/dl	102 (73–154)
Median lipoprotein (interquartile range)–mg/dl	
B	82 (67–98)
A1	150 (132–171)
A2	38 (34–43)
Median TMAO (interquartile range)–μM	3.4 (2.3–5.8)

All subjects gave written informed consent and the Institutional Review Board of the Cleveland Clinic approved all study protocols. Fasting blood lipid profiles were measured on the Abbott ARCHITECT platform (Abbott Diagnostics, Abbot Park, IL).

sured plasma TMAO levels in a large patient population that consisted of 4007 sequential subjects with largely preserved renal function undergoing elective diagnostic cardiac evaluations [3]. In those studies, we examined the relationship between TMAO levels and risk for both prevalent cardiovascular disease and incident risk for myocardial infarction, stroke, or death within the 3 years following sample collection and observed a hazard ratio for highest vs lowest TMAO quartile of 2.54-fold (95% confidence interval, 1.96

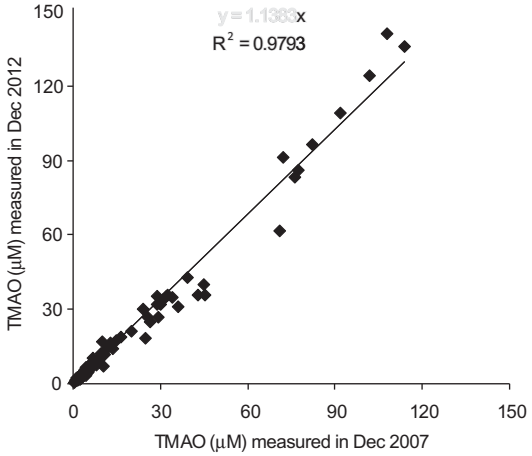

Fig.7. The stability of TMAO in frozen plasma samples after long-term storage (5 years at −80 °C). The same set of 124 human plasma samples (randomly selected from GenBank, a large ($n = 10,000$) and well-characterized tissue repository with longitudinal data from sequential consenting subjects undergoing elective diagnostic left heart catheterization) was measured in December 2007 and in December 2012 by LC/MS/MS. The plasma samples were collected between November 5, 2001, and April 5, 2005, and kept frozen at −80 °C until assay. All plasma samples were defrosted at least 2 times.

Table 4
Evaluation of three QC plasma TMAO concentrations which were subjected to 5 freeze and thaw cycles.

QC Plasma	Plasma TMAO (μM)					CV%	
	Cycle 1	Cycle 2	Cycle 3	Cycle 4	Cycle 5	Intercycle	Intracycle
1	1.61	1.77	1.78	1.75	1.71	4.1	2.6
	1.68	1.77	1.71	1.74	1.80		
2	2.47	2.71	2.99	2.58	2.66	8.8	3.3
	2.38	2.60	2.77	2.65	2.58		
3	15.2	16.2	16.3	15.1	15.3	2.9	3.4
	14.9	15.4	15.2	15.9	15.3		

Plasma were frozen at −80 °C in a dry ice box and thawed to room temperature. The same vial of plasma was subjected to five freeze and thaw cycles. TMAO in each sample at each cycle was measured in duplicate.

to 3.28; $P < 0.001$) [3]. Of note, the extremes of TMAO levels observed within this cardiology clinic cohort are similar (i.e., the 0.5 percentile was 0.63 μM and the 99.5 percentile was 77.2 μM) to those observed in the healthy volunteers reported in the present study. Therefore, most of the plasma TMAO levels that will likely be observed in subjects will be situated within the linearity range, 0.1–200 μM, developed for the present assay. The results of the stability studies shown for TMAO in plasma during storage at −80 °C indicate that analyses of TMAO in archival specimens of long duration will be a reliable indicator of the TMAO levels. Although TMAO can work as electron acceptor in bacterium [12,13], its oxidative potential is very limited. Thus, it is perhaps not surprising that the present study demonstrates negligible impact of multiple freeze–thaw cycles on TMAO levels, attesting to the stability of this analyte in sterile complex biological matrices. Thus, TMAO does not readily undergo spontaneous degradation, and alternatively, trimethylamine-containing precursors such as choline, phosphatidylcholine, and carnitine do not readily contribute to the formation of TMAO during storage. The accuracy, precision, and high-throughput nature of the presently described LC/MS/MS assay should greatly facilitate the exploration of the clinical utility of this unique and interesting biomarker of human health and disease.

Competing financial interests

Drs. Hazen, Wang, and Levison report being listed as co-inventor on pending and issued patents held by the Cleveland Clinic relating to cardiovascular diagnostics and therapeutics. Dr. Hazen reports having been paid as a consultant for the following companies: AstraZeneca Pharmaceuticals LP, BG Medicine, Inc., Cleveland Heart Lab, Esperion, Lilly, Liposcience, Inc., Merck & Co., Inc., Pfizer, Inc., and Proctor & Gamble, and Takeda. Dr. Hazen reports receiving research funds from Cleveland Heart Lab, Liposcience, Inc., Proctor & Gamble, and Takeda. Dr. Hazen reports having the right to receive royalty payments for inventions or discoveries related to cardiovascular diagnostics and therapeutics for the companies shown below: Cleveland Heart Lab., Frantz Biomarkers, LLC, Liposcience, Inc. Drs. Levison and Wang report having the right to receive royalty payments for inventions or discoveries related to cardiovascular diagnostics from Liposcience, Inc., and Proctor & Gamble.

Acknowledgments

S.L.H. is supported by United States National Institutes of Health (NIH) and Office of Dietary Supplement Grant R01 HL103866, and NIH Grant P20 HL113452. S.L.H. is also partially supported by a gift from the Leonard Krieger Fund. Z.W. is partially supported by an American Heart Association Scientist Development Grant (12SDG12050473). Mass spectrometry instrumentation used is housed in a facility partially supported by a Center of Innovation Award from AB SCIEX.

References

[1] Z. Wang, E. Klipfell, B.J. Bennett, R. Koeth, B.S. Levison, B. Dugar, A.E. Feldstein, E.B. Britt, X. Fu, Y.M. Chung, Y. Wu, P. Schauer, J.D. Smith, H. Allayee, W.H. Tang, J.A. DiDonato, A.J. Lusis, S.L. Hazen, Gut flora metabolism of phosphatidylcholine promotes cardiovascular disease, Nature 472 (2011) 57–63.

[2] R.A. Koeth, Z. Wang, B.S. Levison, J.A. Buffa, E. Org, B.T. Sheehy, E.B. Britt, X. Fu, Y. Wu, L. Li, J.D. Smith, J.A. DiDonato, J. Chen, H. Li, G.D. Wu, J.D. Lewis, M. Warrier, J.M. Brown, R.M. Krauss, W.H. Tang, F.D. Bushman, A.J. Lusis, S.L. Hazen, Intestinal microbiota metabolism of L-carnitine, a nutrient in red meat, promotes atherosclerosis, Nat. Med. 19 (2013) 576–585.

[3] W.H. Tang, Z. Wang, B.S. Levison, R.A. Koeth, E.B. Britt, X. Fu, Y. Wu, S.L. Hazen, Intestinal microbial metabolism of phosphatidylcholine and cardiovascular risk, N. Engl. J. Med. 368 (2013) 1575–1584.

[4] K.A. daCosta, J.J. Vrbanac, S.H. Zeisel, The measurement of dimethylamine, trimethylamine, and trimethylamine N-oxide using capillary gas chromatography–mass spectrometry, Anal. Biochem. 187 (1990) 234–239.

[5] O.A. Mamer, L. Choiniere, E.P. Treacy, Measurement of trimethylamine and trimethylamine N-oxide independently in urine by fast atom bombardment mass spectrometry, Anal. Biochem. 276 (1999) 144–149.

[6] O.A. Mamer, L. Choiniere, A. Lesimple, Measurement of urinary trimethylamine and trimethylamime oxide by direct infusion electrospray quadrupole time-of-flight mass spectrometry, Anal. Biochem. 406 (2010) 80–82.

[7] M.E. Erupe, A. Liberman-Martin, P.J. Silva, Q.G. Malloy, N. Yonis, D.R. Cocker 3rd, K.L. Purvis-Roberts, Determination of methylamines and trimethylamine-N-oxide in particulate matter by non-suppressed ion chromatography, J. Chromatogr. A 1217 (2010) 2070–2073.

[8] J.D. Bell, J.A. Lee, H.A. Lee, P.J. Sadler, D.R. Wilkie, R.H. Woodham, Nuclear magnetic resonance studies of blood plasma and urine from subjects with chronic renal failure: identification of trimethylamine-N-oxide, Biochim. Biophys. Acta 1096 (1991) 101–107.

[9] B.J. Bennett, T.Q. de Aguiar Vallim, Z. Wang, D.M. Shih, Y. Meng, J. Gregory, H. Allayee, R. Lee, M. Graham, R. Crooke, P.A. Edwards, S.L. Hazen, A.J. Lusis, Trimethylamine-N-oxide, a metabolite associated with atherosclerosis, exhibits complex genetic and dietary regulation, Cell Metab. 17 (2013) 49–60.

[10] B.S. Levison, R. Zhang, Z. Wang, X. Fu, J.A. DiDonato, S.L. Hazen, Quantification of fatty acid oxidation products using online high-performance liquid chromatography tandem mass spectrometry, Free Radic. Biol. Med. 59 (2013) 2–13.

[11] Z. Wang, W.H. Tang, L. Cho, D.M. Brennan, S.L. Hazen, Targeted metabolomic evaluation of arginine methylation and cardiovascular risks: potential mechanisms beyond nitric oxide synthase inhibition, Arterioscler. Thromb. Vasc. Biol. 29 (2009) 1383–1391.

[12] A.R. Strom, J.A. Olafsen, H. Larsen, Trimethylamine oxide: a terminal electron acceptor in anaerobic respiration of bacteria, J. Gen. Microbiol. 112 (1979) 315–320.

[13] E. Stenberg, O.B. Styrvold, A.R. Strom, Trimethylamine oxide respiration in *Proteus* sp. strain NTHC153: electron transfer-dependent phosphorylation and L-serine transport, J. Bacteriol. 149 (1982) 22–28.